Extension of the LS-STAG cut-cell immersed boundary method for RANS-based turbulence models

Valeria V. Puzikova Ilia K. Marchevsky
valeria.puzikova@gmail.com

Abstract

The general approach to the application of the LS-STAG method for the numerical solution of RANS equations is suggested by constructing the LS-STAG method extension with the Spalart — Allmaras turbulent model. According to the concept of the LS-STAG method normal Reynolds stress components are sampled on the base mesh (similar to pressure discretization) and shear ones are sampled in the upper right corners of the base mesh cells. Thus, for the shear Reynolds stresses an additional mesh (xy-mesh) is introduced. In case of Reynolds Stress (RSM) RANS models, these meshes are used for transport equation solving for Reynolds stresses. The result then is taken into account in the Helmholtz equation for the velocity. In case of Eddy Viscosity (EVM) RANS models eddy viscosity is sampled on the xy-mesh. In this research the LS-STAG-discretization for convective and diffusive fluxes on the additional xy-mesh is developed. To validate this approach the flow past circular airfoil at the Reynolds numbers $\mathrm{Re} = 1000$ and $\mathrm{Re} = 3900$ was simulated.

1 Introduction

The LS-STAG method [1] for viscous incompressible flows simulation combines the advantages of the MAC method, immersed boundary methods and level-set method. This method allows to solve on the Cartesian meshes problems when domain shape is irregular or it changes in the simulation process due to hydroelastic body motion. For these reasons, the LS-STAG method is very useful for solving such complicated problems of computational mechanics as coupled hydroelastic problems, biomechanic problems, problems of solid mechanics with deformable bodies. However, the LS-STAG method, as all mesh methods has a significant limitation when simulating flows with high Reynolds number: it requires extremely small space and time steps. It leads to significant increase in computational cost. The traditional method of solving this problem is RANS, LES, DES etc. turbulence models usage. Extension of the LS-STAG method for RANS-based turbulence models is presented in this research.

2 Governing equations

The problem is considered in 2D unsteady case when the flow around an airfoil assumed to be viscous and incompressible. The flow is described by RANS equations:

$$\nabla \cdot \mathbf{v} = 0, \quad \frac{\partial \mathbf{v}}{\partial t} + (\mathbf{v} \cdot \nabla)\mathbf{v} = \frac{1}{\rho}\nabla p + \nu \Delta \mathbf{v} + \nabla \cdot \hat{\tau}^{\,t}.$$

The boundary conditions are the following:

$$\mathbf{v}\big|_{\text{inlet}} = \mathbf{v}_\infty, \quad \frac{\partial \mathbf{v}}{\partial \mathbf{n}}\Big|_{\text{outlet}} = 0, \quad \mathbf{v}\big|_{\text{airfoil}} = \mathbf{0}, \quad \frac{\partial p}{\partial \mathbf{n}}\Big|_{\text{inlet \& outlet \& airfoil}} = 0.$$

In case of Reynolds Stress (RSM) RANS models, for example DRSM, ARSM, EARSM, the Reynolds stress transport equation is solved for simulating of $\hat{\tau}^t$. In case of Eddy Viscosity (EVM) RANS models the eddy viscosity ν^t (and the turbulent kinetic energy k in case of two-equation models) is simulated and Reynolds stresses are evaluated using the Boussinesq eddy viscosity assumption [2].

In Spallart — Allmaras (S-A) turbulence model [3] the eddy viscosity is given by the following equations

$$\begin{gathered}
\nu^t = \tilde{\nu} f_{\nu 1}, \quad \frac{\partial \tilde{\nu}}{\partial t} + (\mathbf{v}\cdot\nabla)\tilde{\nu} = P^\nu - D^\nu + \frac{1}{\sigma}\nabla\cdot[(\nu+\tilde{\nu})\nabla\tilde{\nu}] + \frac{c_{b2}}{\sigma}(\nabla\tilde{\nu})^2, \\
P^\nu - D^\nu = c_{b1}[1-f_{t2}]\tilde{S}\tilde{\nu} - \left(c_{w1}f_w - \frac{c_{b1}}{\varkappa^2}f_{t2}\right)\left(\frac{\tilde{\nu}}{d}\right)^2, \\
f_{\nu 1} = \frac{\chi^3}{\chi^3 + c_{\nu 1}^3}, \ f_{\nu 2} = 1 - \frac{\chi}{1+\chi f_{\nu 1}}, \ f_{t2} = c_{t3}\cdot e^{-c_{t4}\chi^2}, \ f_w = g\left(\frac{1+c_{w3}^6}{g^6+c_{w3}^6}\right)^{1/6}, \\
\chi = \frac{\tilde{\nu}}{\nu}, \ g = r + c_{w2}(r^6 - r), \ r = \frac{\tilde{\nu}}{\tilde{S}\varkappa^2 d^2}, \ \tilde{S} = \left|\frac{\partial u}{\partial y} - \frac{\partial v}{\partial x}\right| + f_{\nu 2}\frac{\tilde{\nu}}{\varkappa^2 d^2}, \\
\varkappa = 0.41, \ c_{\nu 1} = 7.1, \ c_{b1} = 0.1355, \ c_{b2} = 0.622, \\
\sigma = \frac{2}{3}, \ c_{w1} = \frac{c_b 1}{\varkappa^2} + \frac{1+c_{b2}}{\sigma}, \ c_{w2} = 0.3, \ c_{w3} = 2, \ c_{t3} = 1.2, \ c_{t4} = 0.5.
\end{gathered} \tag{1}$$

Here $\tilde{\nu}$ is the S-A working variable, d is the distance from the field point to the nearest wall, P^ν is the production term, D^ν is the destruction term.

The 'Trip-Less' (TL) approach is used: firstly very high value of the S-A working variable is setted on inlet boundary and then once a separation zone is formed value of the S-A working variable on inlet boundary is greatly reduced. Thus, the boundary conditions for (1) take the following form:

$$\tilde{\nu}|_{\text{airfoil}} \equiv 0, \quad \frac{\partial \tilde{\nu}}{\partial \underline{n}}\Big|_{\text{outlet}} = 0, \quad \tilde{\nu}|_{\text{inlet}} = \tilde{\nu}_\infty(t) = \begin{cases} \nu, \ t \le t^*, \\ 0.001\nu, \ t > t^*. \end{cases}$$

3 The LS-STAG method

The Cartesian mesh with cells $\Omega_{i,j} = (x_{i-1}, x_i)\times(y_{j-1}, y_j)$ is introduced in the rectangular computational domain. It is denoted that $\Gamma_{i,j}$ is the face of $\Omega_{i,j}$ and $\underline{x}^c_{i,j} = (x^c_i, y^c_j)$ is the center of this cell. Unknown components $u_{i,j}$ and $v_{i,j}$ of velocity vector $\mathbf{v}$ are computed in the middle of fluid parts of the cell faces. These points are the centers of control volumes $\Omega^u_{i,j} = (x^c_i, x^c_{i+1})\times(y_{j-1}, y_j)$ and $\Omega^v_{i,j} = (x_{i-1}, x_i)\times(y^c_j, y^c_{j+1})$ with faces $\Gamma^u_{i,j}$ and $\Gamma^v_{i,j}$ respectively (fig. 1).

Cells which the immersed boundary intersects are the so-called 'cut-cells' (fig. 2). These cells contain the solid part together with the liquid one. The level-set function φ [4] is used for immersed boundary Γ^{ib} description. The boundary Γ^{ib} is represented by a line segment on the cut-cell $\Omega_{i,j}$. Location of this segment endpoints is defined by a linear interpolation of the variable $\varphi_{i,j} = \varphi(x_i, y_j)$. The cell-face fraction ratios $\vartheta^u_{i,j}$ and $\vartheta^v_{i,j}$ are introduced. They take values in interval $[0, 1]$ and represent the fluid parts of the east and north faces of $\Gamma_{i,j}$ respectively.

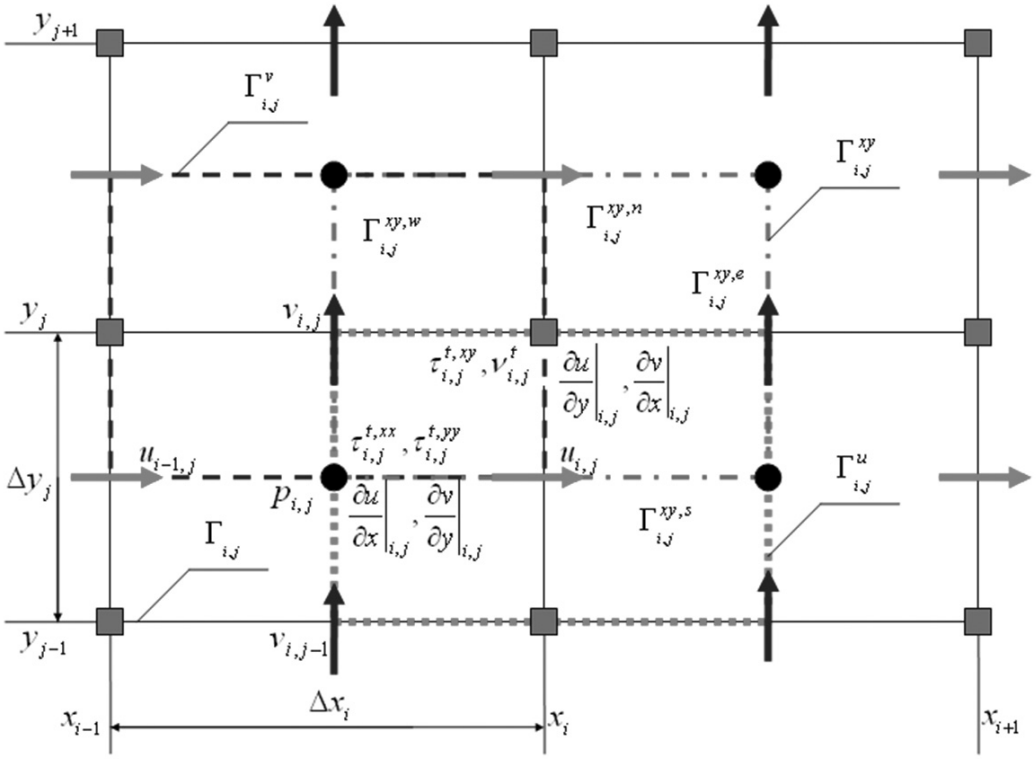

Figure 1: Staggered arrangement of the variables on the LS-STAG mesh

To preserve the five-point structure of the MAC method we need to make distinction between the discretization of the normal and shear stresses (fig. 2). It is proposed to sample the normal and shear Reynolds stresses similarly. It is conveniently to sample the eddy viscosity and the S-A working variable at the same points as the shear stresses. Thus, in case of the LS-STAG method usage for RANS-based models the fourth mesh with cells $\Omega^{xy}_{i,j} = (x^c_i, x^c_{i+1}) \times (y^c_j, y^c_{j+1})$ is needed. The faces of these cells are $\Gamma^{xy}_{i,j}$ (fig. 1) and its volumes are $M^{xy}_{i,j}$. If $i = \overline{1,N}$, $j = \overline{1,M}$, xy-mesh contain $NM_{xy} = (N-1)\cdot(M-1)$ cells.

4 Extension of the LS-STAG method for the Spallart — Allmaras turbulence model

The transport equation (1) in integral form has the following form:

$$\frac{d}{dt}\int\limits_{\Omega^*}\tilde{\nu}\,dV + \int\limits_{\Gamma^*}(\underline{v}\cdot\underline{n})\tilde{\nu}\,dS = \int\limits_{\Omega^*}(P^\nu - D^\nu)\,dV + \frac{1}{\sigma}\int\limits_{\Gamma^*}[\nu+\tilde{\nu}]\nabla\tilde{\nu}\cdot\underline{n}\,dS + \frac{c_{b2}}{\sigma}\int\limits_{\Omega^*}(\nabla\tilde{\nu})^2\,dV. \quad (2)$$

Discretization of $\int\limits_{\Omega^*}(P^\nu - D^\nu)\,dV$ is trivial because production and destruction terms are sampled at the same points as the S-A working variable:

$$\int\limits_{\Omega^{xy}_{i,j}}(P^\nu - D^\nu)\,dV \cong M^{xy}_{i,j}(P^\nu_{i,j} - D^\nu_{i,j}).$$

Convenience of $\tilde{\nu}$ discretization on the xy-mesh consists mainly in the fact that due to this $\partial\tilde{\nu}/\partial x$ and $\partial\tilde{\nu}/\partial y$ are sampled on the y-mesh and x-mesh respectively and they are

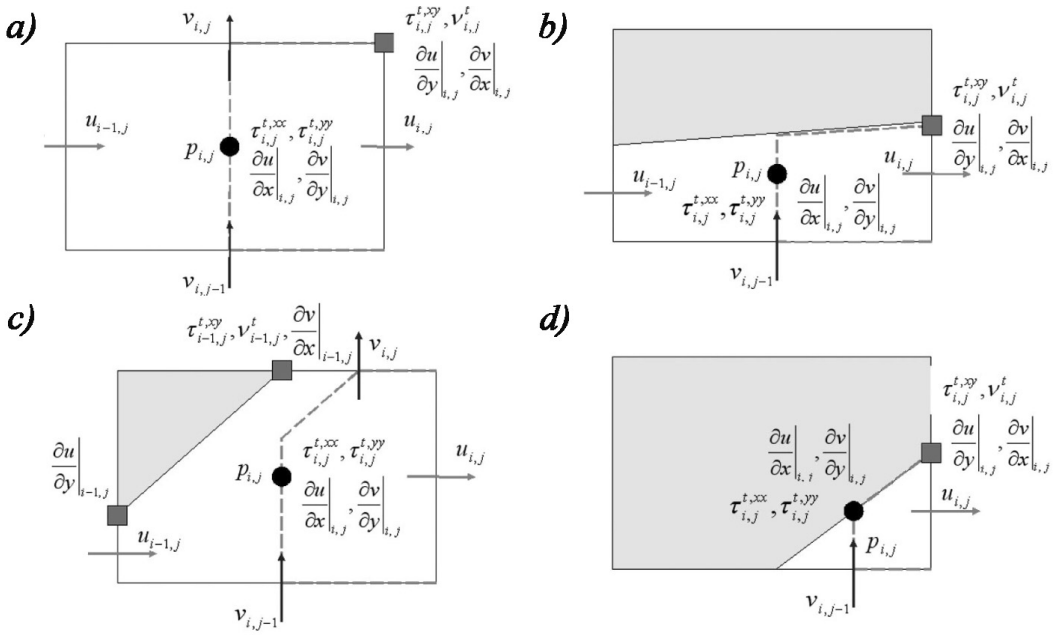

Figure 2: Location of the variables discretization points in the case of generic cells on the LS-STAG mesh: *(a)* Cartesian Fluid Cell; *(b)* North Trapezoidal Cell; *(c)* Northwest Pentagonal Cell; *(d)* Northwest Triangle Cell

calculated using the same formulae for all types of cells:

$$\left.\frac{\partial\tilde{\nu}}{\partial x}\right|_{i,j} = \frac{\tilde{\nu}_{i,j} - \tilde{\nu}_{i-1,j}}{\vartheta^v_{i,j}\Delta x_i}, \quad \left.\frac{\partial\tilde{\nu}}{\partial y}\right|_{i,j} = \frac{\tilde{\nu}_{i,j} - \tilde{\nu}_{i,j-1}}{\vartheta^u_{i,j}\Delta y_j}.$$

Then the discretization of the last term in (2) is the following:

$$\int_{\Omega^{xy}_{i,j}} (\nabla\tilde{\nu})^2\, dV \cong \frac{M^{xy}_{i,j}}{2}\left\{\left(\left.\frac{\partial\tilde{\nu}}{\partial x}\right|_{i,j}\right)^2 + \left(\left.\frac{\partial\tilde{\nu}}{\partial x}\right|_{i+1,j}\right)^2 + \left(\left.\frac{\partial\tilde{\nu}}{\partial y}\right|_{i,j}\right)^2 + \left(\left.\frac{\partial\tilde{\nu}}{\partial y}\right|_{i,j+1}\right)^2\right\} = M^{xy}_{i,j} S^G_{i,j}.$$

For the diffusive term we obtain

$$\begin{aligned}\int_{\Gamma^{xy}_{i,j}} [\nu+\tilde{\nu}]\nabla\tilde{\nu}\cdot\underline{n}\, dS \cong & \left.\frac{\partial\tilde{\nu}}{\partial x}\right|_{i+1,j}\left(\nu + \frac{\tilde{\nu}_{i,j}+\tilde{\nu}_{i+1,j}}{2}\right) - \left.\frac{\partial\tilde{\nu}}{\partial x}\right|_{i,j}\left(\nu + \frac{\tilde{\nu}_{i,j}+\tilde{\nu}_{i-1,j}}{2}\right) + \\ & + \left.\frac{\partial\tilde{\nu}}{\partial y}\right|_{i,j+1}\left(\nu + \frac{\tilde{\nu}_{i,j}+\tilde{\nu}_{i,j+1}}{2}\right) - \left.\frac{\partial\tilde{\nu}}{\partial y}\right|_{i,j}\left(\nu + \frac{\tilde{\nu}_{i,j}+\tilde{\nu}_{i,j-1}}{2}\right).\end{aligned}$$

Then $K^{xy} \in M(\mathbb{R})_{NM_{xy}\times NM_{xy}}$ and $S^{\nu}_{xy} \in \mathbb{R}^{NM_{xy}}$ can be defined:

$$\begin{aligned}\int_{\Gamma^{xy}_{i,j}} [\nu+\tilde{\nu}]\nabla\tilde{\nu}\cdot\underline{n}\, dS \cong\ & K^{xy}_S(i,j)\tilde{\nu}_{i,j-1} + K^{xy}_W(i,j)\tilde{\nu}_{i-1,j} + K^{xy}_P(i,j)\tilde{\nu}_{i,j} + \\ & + K^{xy}_E(i,j)\tilde{\nu}_{i+1,j} + K^{xy}_N(i,j)\tilde{\nu}_{i,j+1} + S^{\nu}_{xy,\ i,j}.\end{aligned}$$

Similarly, the LS-STAG discretization for the convective term on the xy-mesh is obtained:

$$\int\limits_{\Gamma^*} (\underline{v}\cdot\underline{n})\tilde{\nu}\,dS \cong \bar{u}_e\frac{\tilde{\nu}_{i,j}+\tilde{\nu}_{i+1,j}}{2} - \bar{u}_w\frac{\tilde{\nu}_{i,j}+\tilde{\nu}_{i-1,j}}{2} + \bar{v}_n\frac{\tilde{\nu}_{i,j}+\tilde{\nu}_{i,j+1}}{2} - \bar{v}_s\frac{\tilde{\nu}_{i,j}+\tilde{\nu}_{i,j-1}}{2},$$

$$\bar{u}_e = \frac{1}{4}[\vartheta^u_{i,j}u_{i,j}\Delta y_j + \vartheta^u_{i+1,j}u_{i+1,j}\Delta y_j + \vartheta^u_{i,j+1}u_{i,j+1}\Delta y_{j+1} + \vartheta^u_{i+1,j+1}u_{i+1,j+1}\Delta y_{j+1}],$$

$$\bar{u}_w = \frac{1}{4}[\vartheta^u_{i,j}u_{i,j}\Delta y_j + \vartheta^u_{i-1,j}u_{i-1,j}\Delta y_j + \vartheta^u_{i,j+1}u_{i,j+1}\Delta y_{j+1} + \vartheta^u_{i-1,j+1}u_{i-1,j+1}\Delta y_{j+1}],$$

$$\bar{v}_n = \frac{1}{4}[\vartheta^v_{i,j}v_{i,j}\Delta x_i + \vartheta^v_{i,j+1}v_{i,j+1}\Delta x_i + \vartheta^v_{i+1,j}v_{i+1,j}\Delta x_{i+1} + \vartheta^v_{i+1,j+1}v_{i+1,j+1}\Delta x_{i+1}],$$

$$\bar{v}_s = \frac{1}{4}[\vartheta^v_{i,j}v_{i,j}\Delta x_i + \vartheta^v_{i,j-1}v_{i,j-1}\Delta x_i + \vartheta^v_{i+1,j}v_{i+1,j}\Delta x_{i+1} + \vartheta^v_{i+1,j-1}v_{i+1,j-1}\Delta x_{i+1}].$$

This discretization leads to skew-symmetric matrix $C^{xy}\in M(\mathbb{R})_{NM_{xy}\times NM_{xy}}$ as well as on x-mesh and y-mesh because the discrete continuity equation is verified:

$$C^{xy}_S(i,j) = -\bar{v}_s/2,\ C^{xy}_W(i,j) = -\bar{u}_w/2,\ C^{xy}_E(i,j) = \bar{u}_e/2,\ C^{xy}_N(i,j) = \bar{v}_n/2.$$

Additionally, the $S^c_{xy}\in\mathbb{R}^{NM_{xy}}$ contains a non-zero components corresponding the computational domain boundaries:

$$S^c_{xy,\ i,M-2} = \bar{v}_n\tilde{\nu}_\infty/2,\ S^c_{xy,\ i,1} = -\bar{v}_s\tilde{\nu}_\infty/2,\ i=\overline{2,N-3};\ S^c_{xy,\ 1,M-2} = (\bar{v}_n-\bar{u}_w)\tilde{\nu}_\infty/2;$$

$$S^c_{xy,\ 1,j} = -\bar{u}_w\tilde{\nu}_\infty/2,\ S^c_{xy,\ N-2,j} = \bar{u}_e\tilde{\nu}_{N-2,j}/2,\ j=\overline{2,M-3};\ S^c_{xy,\ 1,1} = -(\bar{v}_s+\bar{u}_w)\tilde{\nu}_\infty/2;$$

$$S^c_{xy,\ N-2,M-2} = (\bar{v}_n\tilde{\nu}_\infty + \bar{u}_e\tilde{\nu}_{N-2,M-2})/2,\ S^c_{xy,\ N-2,1} = (-\bar{v}_s\tilde{\nu}_\infty + \bar{u}_e\tilde{\nu}_{N-2,M-2})/2.$$

Thus, the following difference analogue of (2) is obtained:

$$\tilde{\nu}^{n+1} = \tilde{\nu}^n + \Delta t\left[(M^{xy})^{-1}\left\{\frac{K^{xy,n}\tilde{\nu}^n + S^{\nu,n}_{xy}}{\sigma} - C^{xy,n}\tilde{\nu}^n - S^{c,n}_{xy}\right\} + P^{\nu,n} - D^{\nu,n} + \frac{c_{b2}S^{G,n}}{\sigma}\right].$$

Here Δt is the time discretization step.

5 Numerical experiments

The flow past circular airfoil was simulated using the developed modification of the LS-STAG method at the Reynolds numbers Re = 1000 (on non-uniform meshes 120×148 with $\Delta t = 5\cdot10^{-2}$ and 240×296 with $\Delta t = 10^{-3}$) and Re = 3900 (on non-uniform meshes 120×148 with $\Delta t = 10^{-3}$ and 240×296 with $\Delta t = 5\cdot10^{-4}$). The time averaged drag coefficient C_{xa} and the Strouhal number Sh was computed. The coefficient C_{xa} is obtained by averaging over a large period of time the unsteady load $C_{xa}(t) = \dfrac{2F_{xa}}{\rho V^2_\infty}$. Computational results are shown in table 18. These results are in good agreement with experimental data for simulation on coarse meshes by using the proposed modification of the LS-STAG method.

Table 18: Comparison of C_{xa} and Sh with established results from the literature

Turbulence model	Number of cells	Re = 1000		Re = 3900	
		C_{xa}	Sh	C_{xa}	Sh
Experiment [5]		0.98	0.21	0.93	0.215
[6]	—	1.15	—	—	—
LES [7]	1 103 520	—	—	1.08	—
SV LES [8]	30 720	—	—	1.01	0.218
FV LES [8]	855 040	—	—	1.07	0.242
S-A, present study	17 760	1.123	0.26	0.847	0.22
S-A, present study	71 040	1.032	0.25	0.984	0.24
$k-\varepsilon$ [9]	46 304	0.995	0.15	0.997	0.153
Real $k-\varepsilon$ [9]	46 304	—	0.173	—	0.195
SST $k-\omega$ [9]	46 304	—	0.234	—	0.25
$k-\varepsilon$ [10], ANSYS	388 550	1.169	—	0.7446	—
SST $k-\omega$ [10], ANSYS	388 550	0.9891	—	0.6208	—
LES [10], ANSYS	388 550	1.1499	0.21	1.0683	—

6 Conclusion

The key points of the LS-STAG method extension for RANS-based turbulence models were described. For the shear Reynolds stresses and for the eddy viscosity an additional mesh (xy-mesh) is introduced. The general approach to the construction of the LS-STAG discretization for differential equations of the EVM RANS models on the additional xy-mesh shown on the example of the Spalarat — Allmaras model. To validate this approach the flow past a circular airfoil at the Reynolds numbers Re = 1000 and Re = 3900 was simulated. Computational results are in good agreement with established results from the literature.

Acknowledgements

The work was partially supported by Russian Federation President Grant for young scientists [proj. MK-6618.2013.08].

References

[1] Cheny Y., Botella O. The LS-STAG method: A new immersed boundary/level-set method for the computation of incompressible viscous flows in complex moving geometries with good conservation properties// J. Comput. Phys. 2010. N 229. P. 1043–1076.

[2] Spalart P.R. Strategies for turbulence modelling and simulations// Int. J. Heat and Fluid Flow. 2000. N 21. P. 252–263.

[3] Spalart P.R., Allmaras S.R. A One-Equation Turbulence Model for Aerodynamic Flows// Recherche Aerospatiale. 1994. N 1. P. 5–21.

[4] Osher S., Fedkiw R.P. Level set methods and dynamic implicit surfaces. Springer, 2003.

[5] Zdravkovich M.M. Flow around circular cylinders. Oxford University Press, 1997.

[6] Braza M., Chassaing P., Minh H.H. The numerical study and physical analysis of the pressure and velocity fields in the near wake of a circular cylinder// J. Fluid Mech. 1986. N 165. P. 79–130.

[7] Breuer M. Large Eddy Simulation of the subcritical flow past a circular cylinder: numerical and modelling aspects// Int. J. Numer. Meth. Fluids. 1998. N 28. P. 1281–1302.

[8] Blackburn H.M., Schmidt S. Large Eddy Simulation of flow past a circular cylinder// 14th Australasian Fluid Mechanics Conference, Adelaide University, Adelaide, Australia, 2001.

[9] Rahman M.M., Karim M.M., Alim M.A. Numerical investigation of unsteady flow past a circular cylinder using 2-D finite volume method// J. Naval Arch. and Marine Eng. 2007. N 4. P. 27–42.

[10] Patel Y. Numerical Investigation of flow past a circular cylinder and in a staggered tube bundle using various turbulence models. Master's thesis. Lappeenranta: Lappeenranta University of Technology, 2010.

Valeria V. Puzikova, Russia, 105005 Moscow, 2nd Baumanskaya, 5
Ilia K. Marchevsky, Russia, 105005 Moscow, 2nd Baumanskaya, 5